Int. J. Appl. Math. Comput. Sci., 2018, Vol. 28, No. 2, 297–308
DOI: 10.2478/amcs-2018-0021

ROBUST MULTIPLE SENSOR FAULT–TOLERANT CONTROL FOR DYNAMIC NON–LINEAR SYSTEMS: APPLICATION TO THE AERODYNAMICAL TWIN–ROTOR SYSTEM

MARCIN PAZERA [a,*], MARIUSZ BUCIAKOWSKI [a], MARCIN WITCZAK [a]

[a] Institute of Control and Computation Engineering
University of Zielona Góra, ul. Szafrana 2, 65-516 Zielona Góra, Poland
e-mail: {M.Pazera,M.Buciakowski,M.Witczak}@issi.uz.zgora.pl

The paper deals with the problem of designing sensor-fault tolerant control for a class of non-linear systems. The scheme is composed of a robust state and fault estimator as well as a controller. The estimator aims at recovering the real system state irrespective of sensor faults. Subsequently, the fault-free state is used for control purposes. Also, the robust sensor fault estimator is developed in a such a way that a level of disturbances attenuation can be reached pertaining to the fault estimation error. Fault-tolerant control is designed using similar criteria. Moreover, a separation principle is proposed, which makes it possible to design the fault estimator and control separately. The final part of the paper is devoted to the comprehensive experimental study related to the application of the proposed approach to a non-linear twin-rotor system, which clearly exhibits the performance of the new strategy.

Keywords: fault-tolerant control, sensor fault, fault estimation, twin-rotor system.

1. Introduction

As emerging subjects of modern control engineering, fault diagnosis (FD) and fault-tolerant control (FTC) receive constantly growing attention. Just to name a few, the work of Isermann (2011) deals with the software- and hardware-like redundancy based FTC. The book by Mahmoud *et al*. (2003) deals with passive FTC under inaccurate FD. There are also approaches that deal with the fault estimation issue using combined analytical and soft computing strategies (Witczak, 2014; Mrugalski, 2014). Another important problem is the fact that in real applications it is not easy to apply the existing FDI schemes because of the presence of uncertainties, disturbances, and noise (Witczak, 2014). In addition, it is not always possible to get information about disturbances and noise acting on the system. It should be also underlined that the use of on-line fault estimation is essential for all active fault compensation approaches.

A number of suitable fault estimation methods, essentially observer-based (Aouaouda *et al*., 2015; López-Estrada *et al*., 2015; Byrski and Byrski, 2016), Kalman filter-based (Foo *et al*., 2013; Pourbabaee *et al*., 2016), or parameter identification-based (Cai *et al*., 2016) are used. In the work of Seron and De Doná (2015), a fault estimation scheme for non-linear systems that can be modeled in a linear parameter varying form is presented. The max-plus algebra is proposed by Seybold *et al*. (2015) and Majdzik *et al*. (2016) to deal with the fault-tolerant control problem. In the work of Tabatabaeipour and Bak (2014), an observer scheme that simultaneously estimates the state and a fault is considered. Witczak *et al*. (2015) present a robust fault estimation approach for non-linear discrete-time systems using an unknown input observer.

A class of non-linear systems of special attention is the so-called Lipschitz one (Nguyen and Trinh, 2016b; 2016a), in which the mathematical model of the system satisfies the Lipschitz continuity condition. Many observer-based FDI approaches have been reported for this class of non-linear systems, such as unknown input observers (Zhang *et al*., 2015), adaptive observers (Defoort *et al*., 2016), descriptor system approaches (Zhang *et al*., 2014a), and high-gain observers (Khalil and Praly, 2014). In the work of He and Liu (2014), a sliding mode observer has been designed for non-linear Lipschitz bounded systems, and recently, non-linear observers for one-sided Lipschitz systems have been considered (see,

*Corresponding author

e.g., Li *et al.*, 2014; Zhang *et al.* , 2014b; Song, 2015).

It is important to underline that the above works consider unknown but bounded disturbances, which constitute the main source of uncertainty. The non-linearity is treated as a disturbance, which is suitably decoupled. A further extension of the above general framework was recently proposed by Nguyen and Trinh (2016b). In contrast to the approach by Ha and Trinh (2004), the usual Lipschitz condition is replaced here by one-sided and quadratically inner-bounded ones, which extends its applicability to a wider class of non-linear systems. A similar strategy was realized for a reduced-order observer by Nguyen and Trinh (2016a). Taking into account the fact that the estimated unknown input can be perceived as unknown faults, the above approach can be adapted for simultaneous state and fault estimation.

Thus, the objective of this paper is to propose a novel approach to simultaneous state and sensor fault estimation, which can be applied for the purpose of FTC. It is worth mentioning that the proposed technique for state and fault reconstruction is different from the one presented by Witczak *et al.* (2015) where the objective was to determine an optimal state and actuator fault estimation in the sense of the $\mathcal{H}_\infty$ norm. This work is solely devoted to sensor fault estimation with an application to FTC. Sufficient conditions for the existence and stability of the proposed state and actuator fault estimator are expressed in the form of linear matrix inequalities (LMIs), which can be solved using available computational packages (Löfberg, 2004). Subsequently, the controller design procedure is formed in a similar fashion. Moreover, a separation principle is proposed, which makes it possible to design the state-fault estimator and FTC separately.

The paper is organized as follows. Section 2 presents preliminaries, which are necessary to undertake the problem being investigated. Section 3 proposes a novel strategy for integrated sensor fault estimation and FTC. Section 4 presents application of the proposed strategy to the non-linear twin-rotor system. Finally, the last section concludes the paper.

2. Preliminaries

Let us consider a non-linear discrete-time system:

$$\boldsymbol{x}_{k+1} = \boldsymbol{A}\boldsymbol{x}_k + \boldsymbol{B}\boldsymbol{u}_k + \boldsymbol{g}\left(\boldsymbol{x}_k, \boldsymbol{u}_k\right) + \boldsymbol{W}_1\boldsymbol{w}_k, \quad (1)$$

$$\boldsymbol{y}_k = \boldsymbol{C}\boldsymbol{x}_k + \boldsymbol{f}_{s,k} + \boldsymbol{W}_2\boldsymbol{w}_k, \quad (2)$$

where $\boldsymbol{x}_k \in \mathbb{X} \subset \mathbb{R}^n$, $\boldsymbol{u}_k \in \mathbb{R}^r$, $\boldsymbol{y}_k \in \mathbb{R}^m$, are the state, control input and output vectors, respectively. The non-linear function $\boldsymbol{g}\left(\boldsymbol{x}_k, \boldsymbol{u}_k\right)$ describes the behaviour of the system with respect to the state and input. Moreover $\boldsymbol{f}_{s,k} \in \mathbb{F}_s \subset \mathbb{R}^m$ is the sensor fault vector. Furthermore, $\boldsymbol{W}_1$ and $\boldsymbol{W}_2$ denote distribution matrices of an exogenous disturbance vector $\boldsymbol{w}_k$ obeying

$$l_2 = \{\mathbf{w} \in \mathbb{R}^n | \ \|\mathbf{w}\|_{l_2} < +\infty\}, \quad (3)$$

$$\|\mathbf{w}\|_{l_2} = \left(\sum_{k=0}^{\infty} \|\boldsymbol{w}_k\|^2\right)^{\frac{1}{2}}. \quad (4)$$

It can be easily shown that $\boldsymbol{w}_k$ can be split in such a way as

$$\boldsymbol{w}_k = \left[\boldsymbol{w}_{1,k}^T, \boldsymbol{w}_{2,k}^T\right]^T,$$

where $\boldsymbol{w}_{1,k}$ and $\boldsymbol{w}_{2,k}$ are process and measurement uncertainties, respectively.

The problem is to control the system irrespective of the sensor faults. An integrated strategy of control and fault diagnosis should be able to tolerate the sensor faults, which may occur in the system. The general idea behind this approach is to estimate the faults. Based on this knowledge, the state estimate can be used to guide the system towards a fault-free behaviour.

For further derivations, let us recall the following result (de Oliveira *et al.*, 1999).

Lemma 1. *The following statements are equivalent:*

1. *There exist* $\boldsymbol{X} \succ 0$ *and* $\boldsymbol{W} \succ 0$ *such that*

$$\boldsymbol{V}_i^T\boldsymbol{X}\boldsymbol{V}_i - \boldsymbol{W} \prec 0. \quad (5)$$

2. *There exist* $\boldsymbol{X} \succ 0$, $\boldsymbol{W} \succ 0$ *and* $\boldsymbol{U}$ *such that*

$$\begin{bmatrix} -\boldsymbol{W} & \boldsymbol{V}_i^T\boldsymbol{U}^T \\ \boldsymbol{U}\boldsymbol{V}_i & \boldsymbol{X} - \boldsymbol{U} - \boldsymbol{U}^T \end{bmatrix} \prec 0. \quad (6)$$

Remark 1. For the purpose of further deliberations, it is important to note that the regularity of $\boldsymbol{U}$ implies $\boldsymbol{U} + \boldsymbol{U}^T \succ \boldsymbol{X} \succ \boldsymbol{0}$. Thus, the existence of (6) implies that it is possible to calculate $\boldsymbol{U}^{-1}$.

3. Sensor FTC strategy

The main objective of this section is to design a controller and a fault estimator which will make it possible to estimate all states and sensor faults as well as to compensate the fault effect. As a consequence, it allows controling the system in a faulty sensor case.

3.1. Sensor fault estimator. The following state and sensor fault estimator is proposed:

$$\begin{aligned} \hat{\boldsymbol{x}}_{k+1} &= \boldsymbol{A}\hat{\boldsymbol{x}}_k + \boldsymbol{B}\boldsymbol{u}_k + \boldsymbol{g}\left(\hat{\boldsymbol{x}}_k, \boldsymbol{u}_k\right) \\ &\quad + \boldsymbol{K}_x\left(\boldsymbol{y}_k - \boldsymbol{C}\hat{\boldsymbol{x}}_k - \hat{\boldsymbol{f}}_{s,k}\right), \end{aligned} \quad (7)$$

$$\hat{\boldsymbol{f}}_{s,k+1} = \hat{\boldsymbol{f}}_{s,k} + \boldsymbol{K}_s\left(\boldsymbol{y}_k - \boldsymbol{C}\hat{\boldsymbol{x}}_k - \hat{\boldsymbol{f}}_{s,k}\right), \quad (8)$$

where $\hat{\boldsymbol{x}}_k$ and $\hat{\boldsymbol{f}}_{s,k}$ are state and fault estimates, respectively.

Instead of using a set of observers, the idea is to use one single observer (7)–(8) to estimate all sensor faults.

The problem is to find $\boldsymbol{K}_x$ and $\boldsymbol{K}_s$ which represent gain matrices for the state and fault estimate, respectively. To handle this issue, from (1)–(7) a state estimation error can be derived as

$$\begin{aligned} \boldsymbol{e}_{k+1} &= \boldsymbol{x}_{k+1} - \hat{\boldsymbol{x}}_{k+1} \\ &= \boldsymbol{A}\boldsymbol{x}_k + \boldsymbol{B}\boldsymbol{u}_k + \boldsymbol{g}\left(\boldsymbol{x}_k, \boldsymbol{u}_k\right) \\ &\quad + \boldsymbol{W}_1\boldsymbol{w}_k - \boldsymbol{A}\hat{\boldsymbol{x}}_k - \boldsymbol{B}\boldsymbol{u}_k - \boldsymbol{g}\left(\hat{\boldsymbol{x}}_k, \boldsymbol{u}_k\right) \\ &\quad - \boldsymbol{K}_x\boldsymbol{y}_k + \boldsymbol{K}_x\boldsymbol{C}\hat{\boldsymbol{x}}_k + \boldsymbol{K}_x\hat{\boldsymbol{f}}_{s,k} \\ &= \left[\boldsymbol{A} - \boldsymbol{K}_x\boldsymbol{C}\right]\boldsymbol{e}_k + \boldsymbol{g}\left(\boldsymbol{x}_k, \boldsymbol{u}_k\right) - \boldsymbol{g}\left(\hat{\boldsymbol{x}}_k, \boldsymbol{u}_k\right) \\ &\quad - \boldsymbol{K}_x\boldsymbol{e}_{s,k} + \left[\boldsymbol{W}_1 - \boldsymbol{K}_x\boldsymbol{W}_2\right]\boldsymbol{w}_k, \end{aligned} \tag{9}$$

where $\boldsymbol{e}_{s,k} = \boldsymbol{f}_{s,k} - \hat{\boldsymbol{f}}_{s,k}$ is the fault estimation error. Subsequently, using (2) and (8), the fault estimation error can be rewritten as follows

$$\begin{aligned} \boldsymbol{e}_{s,k+1} &= \boldsymbol{f}_{s,k+1} - \hat{\boldsymbol{f}}_{s,k+1} \\ &= \boldsymbol{f}_{s,k+1} + \boldsymbol{f}_{s,k} - \boldsymbol{f}_{s,k} - \hat{\boldsymbol{f}}_{s,k} \\ &\quad - \boldsymbol{K}_s\boldsymbol{y}_k + \boldsymbol{K}_s\boldsymbol{C}\hat{\boldsymbol{x}}_k + \boldsymbol{K}_s\hat{\boldsymbol{f}}_{s,k} \\ &= \boldsymbol{\varepsilon}_k + \left[\boldsymbol{I} - \boldsymbol{K}_s\right]\boldsymbol{e}_{s,k} \\ &\quad - \boldsymbol{K}_s\boldsymbol{C}\boldsymbol{e}_k - \boldsymbol{K}_s\boldsymbol{W}_2\boldsymbol{w}_k, \end{aligned} \tag{10}$$

with $\boldsymbol{\varepsilon}_k = \boldsymbol{f}_{s,k+1} - \boldsymbol{f}_{s,k}$. For the purpose of further deliberations it is assumed that $\boldsymbol{\varepsilon}_k \in l_2$.

Using the differential mean value theorem (DMVT) (Zemouche and Boutayeb, 2006) it can be shown that

$$\boldsymbol{g}\left(\boldsymbol{x}_k, \boldsymbol{u}_k\right) - \boldsymbol{g}\left(\hat{\boldsymbol{x}}_k, \boldsymbol{u}_k\right) = \boldsymbol{M}_k\left(\boldsymbol{x}_k - \hat{\boldsymbol{x}}_k\right), \tag{11}$$

with

$$\boldsymbol{M}_k = \begin{bmatrix} \dfrac{\partial g_1}{\partial x}(\boldsymbol{c_1}, \boldsymbol{u_k}) \\ \vdots \\ \dfrac{\partial g_n}{\partial x}(\boldsymbol{c_n}, \boldsymbol{u_k}) \end{bmatrix}, \tag{12}$$

where $\boldsymbol{c}_1, \dots, \boldsymbol{c}_n \in \mathrm{Co}(\boldsymbol{x_k}, \hat{\boldsymbol{x}}_{\boldsymbol{k}})$, $\boldsymbol{c}_i \neq \boldsymbol{x_k}$, $\boldsymbol{c}_i \neq \hat{\boldsymbol{x}}_{\boldsymbol{k}}$, $i = 1, \dots, n$. Having in mind the fact that all states are bounded in a real system, $\boldsymbol{x}_k \in \mathbb{X}$ satisfies

$$\underline{x}_{i,j} \leq \frac{\partial \boldsymbol{g}_i(\boldsymbol{x})}{\partial x_j} \leq \bar{x}_{i,j}, \qquad i = 1, \dots, n, \quad j = 1, \dots, n, \tag{13}$$

and hence it is clear that there exist $\boldsymbol{M}_k \in \mathbb{M}$ such that

$$\mathbb{M} = \Big\{\boldsymbol{M}_k \in \mathbb{R}^{n\times n} | \underline{x}_{i,j} \leq m_{k,i,j} \leq \bar{x}_{i,j}, \quad i, j = 1, \dots, n, \Big\}. \tag{14}$$

Thus, the state estimation error (9) can be rewritten in the following form:

$$\begin{aligned} \boldsymbol{e}_{k+1} &= \boldsymbol{x}_{k+1} - \hat{\boldsymbol{x}}_{k+1} \\ &= \left[\boldsymbol{A} + \boldsymbol{M}_k - \boldsymbol{K}_x\boldsymbol{C}\right]\boldsymbol{e}_k \\ &\quad - \boldsymbol{K}_x\boldsymbol{e}_{s,k} + \left[\boldsymbol{W}_1 - \boldsymbol{K}_x\boldsymbol{W}_2\right]\boldsymbol{w}_k. \end{aligned} \tag{15}$$

By defining

$$\bar{\boldsymbol{e}}_{k+1} = \begin{bmatrix} \boldsymbol{e}_{k+1} \\ \boldsymbol{e}_{s,k+1} \end{bmatrix}, \quad \boldsymbol{v}_k = \begin{bmatrix} \boldsymbol{w}_k \\ \boldsymbol{\varepsilon}_k \end{bmatrix}, \tag{16}$$

it can be shown that the state and fault estimation error can be presented in a compact form

$$\begin{aligned} \bar{\boldsymbol{e}}_{k+1} &= \boldsymbol{X}_k\bar{\boldsymbol{e}}_k + \boldsymbol{Z}\boldsymbol{v}_k \\ &= (\bar{\boldsymbol{A}}_k - \bar{\boldsymbol{K}}\bar{\boldsymbol{C}})\bar{\boldsymbol{e}}_k + (\bar{\boldsymbol{W}} - \bar{\boldsymbol{K}}\bar{\boldsymbol{V}})\boldsymbol{v}_k, \end{aligned} \tag{17}$$

where

$$\begin{gathered} \bar{\boldsymbol{A}}_k = \begin{bmatrix} \boldsymbol{A} + \boldsymbol{M}_k & \boldsymbol{0} \\ \boldsymbol{0} & \boldsymbol{I} \end{bmatrix}, \quad \bar{\boldsymbol{C}} = \begin{bmatrix} \boldsymbol{C} & \boldsymbol{I} \end{bmatrix}, \\ \bar{\boldsymbol{W}} = \begin{bmatrix} \boldsymbol{W}_1 & \boldsymbol{0} \\ \boldsymbol{0} & \boldsymbol{I} \end{bmatrix}, \quad \bar{\boldsymbol{V}} = \begin{bmatrix} \boldsymbol{W}_2 & \boldsymbol{0} \end{bmatrix}, \\ \bar{\boldsymbol{K}} = \begin{bmatrix} \boldsymbol{K}_x \\ \boldsymbol{K}_s \end{bmatrix}. \end{gathered} \tag{18}$$

Remark 2. It should be noted that the feasibility of the proposed scheme is dependent on the observability of (1) and (2), which can be impaired by sensors faults. Indeed, the total failure of ith sensor means that $\boldsymbol{f}_{s,i,k} = -\boldsymbol{y}_{i,k}$. In this situation the observation matrix $\boldsymbol{C}$ has its i-th row equal to zero. Thus, the further performance of the proposed scheme depends solely on the observability of (1)–(2) under the updated observation matrix $\boldsymbol{C}$. Under such an observability condition, the convergence of (7)–(8) is guaranteed by Theorem 1.

Taking into account the estimation error for both state and fault, the following result is proposed:

Theorem 1. *For a prescribed attenuation level μ_s of $\boldsymbol{v}_k$, the $\mathcal{H}_\infty$ estimator design problem for the system* (1)–(2) *is solvable if there exist $\boldsymbol{N}$, $\boldsymbol{U}$ and $\boldsymbol{P} \succ \boldsymbol{0}$ such that for all $\boldsymbol{M}_k \in \mathbb{M}$, the following condition is satisfied:*

$$\begin{bmatrix} \boldsymbol{I} - \boldsymbol{P} & \boldsymbol{0} & \bar{\boldsymbol{A}}_k^T\boldsymbol{U}^T - \bar{\boldsymbol{C}}^T\boldsymbol{N}^T \\ \boldsymbol{0} & -\mu_s^2\boldsymbol{I} & \bar{\boldsymbol{W}}^T\boldsymbol{U}^T - \bar{\boldsymbol{V}}^T\boldsymbol{N}^T \\ \boldsymbol{U}\bar{\boldsymbol{A}}_k - \boldsymbol{N}\bar{\boldsymbol{C}} & \boldsymbol{U}\bar{\boldsymbol{W}} - \boldsymbol{N}\bar{\boldsymbol{V}} & \boldsymbol{P} - \boldsymbol{U} - \boldsymbol{U}^T \end{bmatrix} \prec 0. \tag{19}$$

Proof. The problem of designing the $\mathcal{H}_\infty$ observer (Li and Fu, 1997; Zemouche *et al.*, 2008) is to obtain matrices $\boldsymbol{N}, \boldsymbol{U}$ and $\boldsymbol{P}$ such that

$$\lim_{k\to\infty} \bar{\boldsymbol{e}}_k = \boldsymbol{0} \quad \text{for } \boldsymbol{v}_k = \boldsymbol{0}, \tag{20}$$

$$\|\bar{\boldsymbol{e}}_k\|_{l_2} < \mu_s\|\boldsymbol{v}_k\|_{l_2} \quad \text{for } \boldsymbol{v}_k \neq \boldsymbol{0},\ \bar{\boldsymbol{e}}_0 = \boldsymbol{0}. \tag{21}$$

To solve the problem, it is satisfactory to find a Lyapunov function such that

$$\Delta V_{s,k} + \bar{\boldsymbol{e}}_k^T\bar{\boldsymbol{e}}_k - \mu_s^2\boldsymbol{v}_k^T\boldsymbol{v}_k < 0, \tag{22}$$

where $\Delta V_{s,k} = V_{s,k+1} - V_{s,k}$, $V_{s,k} = \bar{\boldsymbol{e}}_k^T \boldsymbol{P} \bar{\boldsymbol{e}}_k$ and $\boldsymbol{P} \succ 0$. If $\boldsymbol{v}_k = \boldsymbol{0}$, then the Lyapunov function (22) takes the following simplified form:

$$\Delta V_{s,k} + \bar{\boldsymbol{e}}_k^T \bar{\boldsymbol{e}}_k < 0, \tag{23}$$

and hence $\Delta V_{s,k} < 0$, which leads to (20). If $\boldsymbol{v}_k \neq \boldsymbol{0}$ and we take into account the fact that

$$\sum_{k=0}^{\infty} (\Delta V_{s,k}) = V_{s,\infty} - V_{s,0}, \quad V_{s,\infty} = V_{s,0} = 0,$$

then (22) yields

$$\begin{aligned} &\sum_{k=0}^{\infty} (\Delta V_{s,k}) + \sum_{k=0}^{\infty} \left(\bar{\boldsymbol{e}}_k^T \bar{\boldsymbol{e}}_k\right) - \mu_s^2 \sum_{k=0}^{\infty} \left(\boldsymbol{v}_k^T \boldsymbol{v}_k\right) < 0 \\ &\Longrightarrow -V_0 + \sum_{k=0}^{\infty} \left(\bar{\boldsymbol{e}}_k^T \bar{\boldsymbol{e}}_k\right) - \mu_s^2 \sum_{k=0}^{\infty} \left(\boldsymbol{v}_k^T \boldsymbol{v}_k\right) < 0 \\ &\Longrightarrow \sum_{k=0}^{\infty} \left(\bar{\boldsymbol{e}}_k^T \bar{\boldsymbol{e}}_k\right) - \mu_s^2 \sum_{k=0}^{\infty} \left(\boldsymbol{v}_k^T \boldsymbol{v}_k\right) < 0 \\ &\Longrightarrow \sum_{k=0}^{\infty} \left(\bar{\boldsymbol{e}}_k^T \bar{\boldsymbol{e}}_k\right) < \mu_s^2 \sum_{k=0}^{\infty} \left(\boldsymbol{v}_k^T \boldsymbol{v}_k\right) \\ &\Longrightarrow \|\bar{\boldsymbol{e}}_k\|_{l_2} < \mu_s \|\boldsymbol{v}_k\|_{l_2}, \end{aligned}$$

which leads to (21). As a consequence by using (17) it is easy to show that

$$\begin{aligned} &\Delta V_{s,k} + \bar{\boldsymbol{e}}_k^T \bar{\boldsymbol{e}}_k - \mu_s^2 \boldsymbol{v}_k^T \boldsymbol{v}_k \\ &\quad = \bar{\boldsymbol{e}}_k^T \left(\boldsymbol{X}_k^T \boldsymbol{P} \boldsymbol{X}_k + \boldsymbol{I} - \boldsymbol{P}\right) \bar{\boldsymbol{e}}_k \\ &\quad + \bar{\boldsymbol{e}}_k^T \left(\boldsymbol{X}_k^T \boldsymbol{P} \boldsymbol{Z}\right) \boldsymbol{v}_k \\ &\quad + \boldsymbol{v}_k^T \left(\boldsymbol{Z}^T \boldsymbol{P} \boldsymbol{X}_k\right) \bar{\boldsymbol{e}}_k \\ &\quad + \boldsymbol{v}_k^T \left(\boldsymbol{Z}^T \boldsymbol{P} \boldsymbol{Z} - \mu_s^2 \boldsymbol{I}\right) \boldsymbol{v}_k < 0. \end{aligned} \tag{24}$$

By introducing

$$\bar{\boldsymbol{v}}_k = \begin{bmatrix} \bar{\boldsymbol{e}}_k \\ \boldsymbol{v}_k \end{bmatrix}, \tag{25}$$

it can be shown that (24) can be rewritten in the following form:

$$\bar{\boldsymbol{v}}_k^T \begin{bmatrix} \boldsymbol{X}_k^T \boldsymbol{P} \boldsymbol{X}_k + \boldsymbol{I} - \boldsymbol{P} & \boldsymbol{X}_k^T \boldsymbol{P} \boldsymbol{Z} \\ \boldsymbol{Z}^T \boldsymbol{P} \boldsymbol{X}_k & \boldsymbol{Z}^T \boldsymbol{P} \boldsymbol{Z} - \mu_s^2 \boldsymbol{I} \end{bmatrix} \bar{\boldsymbol{v}}_k \prec 0, \tag{26}$$

which is equivalent to

$$\begin{bmatrix} \boldsymbol{X}_k^T \\ \boldsymbol{Z}^T \end{bmatrix} \boldsymbol{P} \begin{bmatrix} \boldsymbol{X}_k & \boldsymbol{Z} \end{bmatrix} + \begin{bmatrix} \boldsymbol{I} - \boldsymbol{P} & \boldsymbol{0} \\ \boldsymbol{0} & -\mu_s^2 \boldsymbol{I} \end{bmatrix} \prec 0. \tag{27}$$

Applying Lemma 1 to (27) gives

$$\begin{bmatrix} \boldsymbol{I} - \boldsymbol{P} & \boldsymbol{0} & \boldsymbol{X}_k^T \boldsymbol{U}^T \\ \boldsymbol{0} & -\mu_s^2 \boldsymbol{I} & \boldsymbol{Z}^T \boldsymbol{U}^T \\ \boldsymbol{U} \boldsymbol{X}_k & \boldsymbol{U} \boldsymbol{Z} & \boldsymbol{P} - \boldsymbol{U} - \boldsymbol{U}^T \end{bmatrix} \prec 0. \tag{28}$$

Substituting

$$\boldsymbol{U} \boldsymbol{X}_k = \boldsymbol{U} \bar{\boldsymbol{A}}_k - \boldsymbol{U} \bar{\boldsymbol{K}} \bar{\boldsymbol{C}} = \boldsymbol{U} \bar{\boldsymbol{A}}_k - \boldsymbol{N} \bar{\boldsymbol{C}}, \tag{29}$$

$$\boldsymbol{U} \boldsymbol{Z} = \boldsymbol{U} \bar{\boldsymbol{W}} - \boldsymbol{U} \bar{\boldsymbol{K}} \bar{\boldsymbol{V}} = \boldsymbol{U} \bar{\boldsymbol{W}} - \boldsymbol{N} \bar{\boldsymbol{V}}, \tag{30}$$

completes the proof. ■

Note that $\mathbb{M}$ specified by (14) can be equivalently expressed by

$$\mathbb{M} = \left\{ \boldsymbol{M}(\alpha) : \boldsymbol{M}(\alpha) = \sum_{i=1}^{N} \alpha_i \boldsymbol{M}_k, \sum_{i=1}^{N} \alpha_i = 1, \alpha_i \geq 0 \right\}, \tag{31}$$

where $\boldsymbol{N} = 2^{n^2}$. Note that, this is a general description, which does not take into account that some elements of $\boldsymbol{M}$ may be constant. In such cases, $\boldsymbol{N}$ is given by $\boldsymbol{N} = 2^{(n-c)^2}$, where c stands for the number of constant elements of $\boldsymbol{M}$. Thus, the system can be described in a linear parameter varying (LPV) form. Solving (19) is equivalent to (for $i = 1, \ldots, N$)

$$\begin{bmatrix} \boldsymbol{I} - \boldsymbol{P} & \boldsymbol{0} & \bar{\boldsymbol{A}}_i^T \boldsymbol{U}^T - \bar{\boldsymbol{C}}^T \boldsymbol{N}^T \\ \boldsymbol{0} & -\mu_s^2 \boldsymbol{I} & \bar{\boldsymbol{W}}^T \boldsymbol{U}^T - \bar{\boldsymbol{V}}^T \boldsymbol{N}^T \\ \boldsymbol{U} \bar{\boldsymbol{A}}_i - \boldsymbol{N} \bar{\boldsymbol{C}} & \boldsymbol{U} \bar{\boldsymbol{W}} - \boldsymbol{N} \bar{\boldsymbol{V}} & \boldsymbol{P} - \boldsymbol{U} - \boldsymbol{U}^T \end{bmatrix} \preceq 0. \tag{32}$$

As a result, the gain matrices are obtained as follows:

$$\bar{\boldsymbol{K}} = \begin{bmatrix} \boldsymbol{K}_x \\ \boldsymbol{K}_s \end{bmatrix} = \boldsymbol{U}^{-1} \boldsymbol{N}. \tag{33}$$

3.2. Controller design. Before proceeding with the controller design procedure, it is important to underline the fact, proven in the former section, that the state estimate $\hat{\boldsymbol{x}}_k$ provided by (7) converges to the real state irrespective of sensor faults with the state estimation error given by (10).

Thus, a natural control strategy is

$$\boldsymbol{u}_k = -\boldsymbol{K}_c \hat{\boldsymbol{x}}_k + \boldsymbol{K}_r \boldsymbol{r}_k, \tag{34}$$

where $\boldsymbol{K}_c$, $\boldsymbol{K}_r$ and $\boldsymbol{r}_k$ are a control gain matrix, a pre-filter matrix and a reference vector, respectively. Based on the fault-free state estimate, a classical state feedback controller is proposed. Without loss of generality, let us assume that the reference signal is equal to $\boldsymbol{0}$, and hence, (34) boils down to

$$\boldsymbol{u}_k = -\boldsymbol{K}_c \hat{\boldsymbol{x}}_k. \tag{35}$$

Having in mind that the state estimation error is

$$\boldsymbol{e}_k = \boldsymbol{x}_k - \hat{\boldsymbol{x}}_k, \tag{36}$$

introducing (36) into (35) gives

$$\boldsymbol{u}_k = -\boldsymbol{K}_c \boldsymbol{x}_k + \boldsymbol{K}_c \boldsymbol{e}_k. \tag{37}$$

Substituting the above equation into (1) yields

$$\begin{aligned} \boldsymbol{x}_{k+1} = (\boldsymbol{A} - \boldsymbol{B}\boldsymbol{K}_c)\boldsymbol{x}_k + \boldsymbol{B}\boldsymbol{K}_c\boldsymbol{e}_k \\ + \boldsymbol{g}(\boldsymbol{x}_k, \boldsymbol{u}_k) + \boldsymbol{W}_1\boldsymbol{w}_k. \end{aligned} \tag{38}$$

Let us assume that $\boldsymbol{g}(\boldsymbol{0}, \boldsymbol{u}_k) = \boldsymbol{0}$. Since the system is controlled to the origin, using DMVT and substituting $\hat{\boldsymbol{x}}_k = \boldsymbol{0}$ in (11), it can be shown that

$$\boldsymbol{g}(\boldsymbol{x}_k, \boldsymbol{u}_k) = \boldsymbol{M}_k\boldsymbol{x}_k, \tag{39}$$

with

$$\boldsymbol{M}_k = \begin{bmatrix} \frac{\partial g_1}{\partial x}(\boldsymbol{c_1}, \boldsymbol{u_k}) \\ \vdots \\ \frac{\partial g_n}{\partial x}(\boldsymbol{c_n}, \boldsymbol{u_k}) \end{bmatrix}, \tag{40}$$

Thus, the closed-loop system (38) can be rewritten in the following form:

$$\boldsymbol{x}_{k+1} = \tilde{\boldsymbol{X}}_k\boldsymbol{x}_k + \tilde{\boldsymbol{Y}}\bar{\boldsymbol{e}}_k + \tilde{\boldsymbol{Z}}\boldsymbol{v}_k, \tag{41}$$

where

$$\begin{aligned} \tilde{\boldsymbol{X}}_k &= \tilde{\boldsymbol{A}}_k - \boldsymbol{B}\boldsymbol{K}_c, & \tilde{\boldsymbol{A}}_k &= \boldsymbol{A} + \boldsymbol{M}_k, \\ \tilde{\boldsymbol{Y}} &= [\boldsymbol{B}\boldsymbol{K}_c \;\; \boldsymbol{0}], & \tilde{\boldsymbol{Z}} &= [\boldsymbol{W}_1 \;\; \boldsymbol{0}]. \end{aligned} \tag{42}$$

Remark 3. At this point, an obvious question arises: Is it possible to design the state/fault estimator and controller separately? The objective of the remaining part of this section is to provide a positive answer to this question (*separation principle*) along with suitable design procedure.

Let us start with developing an augmented system composed of (17) and (41) that can be expressed as

$$\begin{bmatrix} \boldsymbol{x}_{k+1} \\ \bar{\boldsymbol{e}}_{k+1} \end{bmatrix} = \begin{bmatrix} \tilde{\boldsymbol{X}}_k & \tilde{\boldsymbol{Y}} \\ \boldsymbol{0} & \boldsymbol{X}_k \end{bmatrix} \begin{bmatrix} \boldsymbol{x}_k \\ \bar{\boldsymbol{e}}_k \end{bmatrix} + \begin{bmatrix} \tilde{\boldsymbol{Z}} & \boldsymbol{0} \\ \boldsymbol{0} & \boldsymbol{Z} \end{bmatrix} \boldsymbol{v}_k. \tag{43}$$

Moreover, define $\tilde{\boldsymbol{z}}_k = \left[\boldsymbol{x}_k^T, \bar{\boldsymbol{e}}_k^T\right]^T$ and

$$\Delta V_k + \tilde{\boldsymbol{z}}_k^T\tilde{\boldsymbol{z}}_k - \mu^2\boldsymbol{v}_k^T\boldsymbol{v}_k < 0, \tag{44}$$

where V_k signifies a Lyapunov function. It can be easily observed from (43) that the *separation principle* holds for $\boldsymbol{v}_k = 0$. Indeed, the convergence of the system is defined by a union of eigenvalue sets of $\tilde{\boldsymbol{X}}_k$ and $\boldsymbol{X}_k$. They can, of course, depend on k, which means that for any k all eigenvalues should lie within a unit circle. In this case, the fault/state estimator and the controller can be designed separately. For $\boldsymbol{v}_k \neq 0$, the fault/state estimator design procedure guarantees that the inequality (22) is satisfied. A similar condition can be defined for the controller:

$$\Delta V_{c,k} + \boldsymbol{x}_k^T\boldsymbol{x}_k - \mu_c^2\boldsymbol{v}_k^T\boldsymbol{v}_k < 0. \tag{45}$$

Thus, if $\Delta V_k = \Delta V_{s,k} + \Delta V_{c,k}$ and (22) as well as (45) are satisfied, then (43) obeys

$$\Delta V_{s,k} + \Delta V_{c,k} + \tilde{\boldsymbol{z}}_k^T\tilde{\boldsymbol{z}}_k - \left(\mu_s^2 + \mu_c^2\right)\boldsymbol{v}_k^T\boldsymbol{v}_k < 0, \tag{46}$$

which is equivalent to (44) with $\mu^2 = \mu_s^2 + \mu_c^2$. The above reasoning clearly shows that the *separation principle* holds for $\boldsymbol{v}_k \neq 0$ as well. As a result, the state feedback controller of the form

$$\boldsymbol{u}_k = -\boldsymbol{K}_c\boldsymbol{x}_k, \tag{47}$$

can be designed in order to satisfy (45).

To solve the controller design problem, the following result is proposed:

Theorem 2. *For a prescribed attenuation level μ_c of $\boldsymbol{v}_k$, the $\mathcal{H}_\infty$ controller design problem for the system (1)–(2) is solvable if there exist $\boldsymbol{N}$, $\boldsymbol{U}$ and $\boldsymbol{P} \succ \boldsymbol{0}$ such that for all $\boldsymbol{M}_k \in \mathbb{M}$, the following condition is satisfied:*

$$\begin{bmatrix} -\boldsymbol{P} & \boldsymbol{0} & \boldsymbol{U}^T\tilde{\boldsymbol{A}}_k^T - \boldsymbol{N}^T\boldsymbol{B}^T & \boldsymbol{U}^T \\ \boldsymbol{0} & -\mu_c^2\boldsymbol{I} & \tilde{\boldsymbol{Z}}^T & \boldsymbol{0} \\ \tilde{\boldsymbol{A}}_k\boldsymbol{U} - \boldsymbol{B}\boldsymbol{N} & \tilde{\boldsymbol{Z}} & \boldsymbol{P} - \boldsymbol{U} - \boldsymbol{U}^T & \boldsymbol{0} \\ \boldsymbol{U} & \boldsymbol{0} & \boldsymbol{0} & -\boldsymbol{I} \end{bmatrix} \prec 0, \tag{48}$$

Proof. The problem of designing the $\mathcal{H}_\infty$ controller is to obtain matrices $\boldsymbol{N}$, $\boldsymbol{U}$ and $\boldsymbol{P}$ such that

$$\lim_{k\to\infty} \boldsymbol{x}_k = \boldsymbol{0} \quad \text{for } \boldsymbol{v}_k = \boldsymbol{0}, \tag{49}$$

$$\|\boldsymbol{x}_k\|_{l_2} \le \mu_c\|\boldsymbol{v}_k\|_{l_2} \quad \text{for } \boldsymbol{v}_k \neq \boldsymbol{0},\ \boldsymbol{x}_0 = \boldsymbol{0}. \tag{50}$$

To solve the problem, it is satisfactory to find a Lyapunov function such that

$$\Delta V_{c,k} + \boldsymbol{x}_k^T\boldsymbol{x}_k - \mu_c^2\boldsymbol{v}_k^T\boldsymbol{v}_k < 0, \tag{51}$$

where $\Delta V_{c,k} = V_{c,k+1} - V_{c,k}$, $V_{c,k} = \boldsymbol{x}_k^T\boldsymbol{U}^{-T}\boldsymbol{P}\boldsymbol{U}^{-1}\boldsymbol{x}_k$, $\boldsymbol{P} \succ \boldsymbol{0}$. In much the some way as for the estimator design, if $\boldsymbol{v}_k = \boldsymbol{0}$, then the Lyapunov function (51) takes the following simplified form:

$$\Delta V_{c,k} + \boldsymbol{x}_k^T\boldsymbol{x}_k < 0, \tag{52}$$

and hence $\Delta V_{c,k} < 0$, which leads to (49). If $\boldsymbol{v}_k \neq \boldsymbol{0}$ and we take into account that

$$\sum_{k=0}^{\infty}(\Delta V_{c,k}) = V_{c,\infty} - V_{c,0}, \quad V_{c,\infty} = V_{c,0} = 0,$$

then (51) yields

$$\begin{aligned}&\sum_{k=0}^{\infty}(\Delta V_{c,k})+\sum_{k=0}^{\infty}\left(\boldsymbol{x}_k^T\boldsymbol{x}_k\right)-\mu_c^2\sum_{k=0}^{\infty}\left(\boldsymbol{v}_k^T\boldsymbol{v}_k\right)<0\\ &\implies -V_0+\sum_{k=0}^{\infty}\left(\boldsymbol{x}_k^T\boldsymbol{x}_k\right)-\mu_c^2\sum_{k=0}^{\infty}\left(\boldsymbol{v}_k^T\boldsymbol{v}_k\right)<0\\ &\implies \sum_{k=0}^{\infty}\left(\boldsymbol{x}_k^T\boldsymbol{x}_k\right)-\mu_c^2\sum_{k=0}^{\infty}\left(\boldsymbol{v}_k^T\boldsymbol{v}_k\right)<0\\ &\implies \sum_{k=0}^{\infty}\left(\boldsymbol{x}_k^T\boldsymbol{x}_k\right)<\mu_c^2\sum_{k=0}^{\infty}\left(\boldsymbol{v}_k^T\boldsymbol{v}_k\right)\\ &\implies \|\boldsymbol{x}_k\|_{l_2}<\mu_c\|\boldsymbol{v}_k\|_{l_2},\end{aligned}$$

which leads to (50). As a consequence by using (41) it is easy to show that

$$\begin{aligned}\Delta V_{c,k}&+\boldsymbol{x}_k^T\boldsymbol{x}_k-\mu_c^2\boldsymbol{v}_k^T\boldsymbol{v}_k\\ &=\boldsymbol{x}_k^T(\tilde{\boldsymbol{X}}_k^T\boldsymbol{U}^{-T}\boldsymbol{P}\boldsymbol{U}^{-1}\tilde{\boldsymbol{X}}_k\\ &\quad+\boldsymbol{I}-\boldsymbol{U}^{-T}\boldsymbol{P}\boldsymbol{U}^{-1})\boldsymbol{x}_k\\ &\quad+\boldsymbol{x}_k^T\left(\tilde{\boldsymbol{X}}_k^T\boldsymbol{U}^{-T}\boldsymbol{P}\boldsymbol{U}^{-1}\tilde{\boldsymbol{Z}}\right)\boldsymbol{v}_k\\ &\quad+\boldsymbol{v}_k^T\left(\tilde{\boldsymbol{Z}}^T\boldsymbol{U}^{-T}\boldsymbol{P}\boldsymbol{U}^{-1}\tilde{\boldsymbol{X}}_k\right)\boldsymbol{x}_k\\ &\quad+\boldsymbol{x}_k^T\left(\tilde{\boldsymbol{Z}}^T\boldsymbol{U}^{-T}\boldsymbol{P}\boldsymbol{U}^{-1}\tilde{\boldsymbol{Z}}-\mu_c^2\boldsymbol{I}\right)\boldsymbol{v}_k<0.\end{aligned} \tag{53}$$

By introducing

$$\breve{\boldsymbol{v}}_{\boldsymbol{k}}=\begin{bmatrix}\boldsymbol{x}_k\\ \boldsymbol{v}_k\end{bmatrix}, \tag{54}$$

it can be shown that (53) can be rewritten to the following form

$$\breve{\boldsymbol{v}}_{\boldsymbol{k}}^T\begin{bmatrix}\boldsymbol{S}_1 & \boldsymbol{S}_2\\ \boldsymbol{S}_3 & \boldsymbol{S}_4\end{bmatrix}\breve{\boldsymbol{v}}_{\boldsymbol{k}}\prec 0, \tag{55}$$

where

$$\begin{aligned}\boldsymbol{S}_1&=\tilde{\boldsymbol{X}}_k^T\boldsymbol{U}^{-T}\boldsymbol{P}\boldsymbol{U}^{-1}\tilde{\boldsymbol{X}}_k+\boldsymbol{I}-\boldsymbol{U}^{-T}\boldsymbol{P}\boldsymbol{U}^{-1},\\ \boldsymbol{S}_2&=\tilde{\boldsymbol{X}}_k^T\boldsymbol{U}^{-T}\boldsymbol{P}\boldsymbol{U}^{-1}\tilde{\boldsymbol{Z}},\\ \boldsymbol{S}_3&=\tilde{\boldsymbol{Z}}^T\boldsymbol{U}^{-T}\boldsymbol{P}\boldsymbol{U}^{-1}\tilde{\boldsymbol{X}}_k,\\ \boldsymbol{S}_4&=\tilde{\boldsymbol{Z}}^T\boldsymbol{U}^{-T}\boldsymbol{P}\boldsymbol{U}^{-1}\tilde{\boldsymbol{Z}}-\mu_c^2\boldsymbol{I},\end{aligned}$$

which is equivalent to

$$\begin{bmatrix}\tilde{\boldsymbol{X}}_k^T\boldsymbol{U}^{-T}\\ \tilde{\boldsymbol{Z}}^T\boldsymbol{U}^{-T}\end{bmatrix}\boldsymbol{P}\begin{bmatrix}\boldsymbol{U}^{-1}\tilde{\boldsymbol{X}}_k & \boldsymbol{U}^{-1}\tilde{\boldsymbol{Z}}\end{bmatrix}+\begin{bmatrix}\boldsymbol{I}-\boldsymbol{U}^{-T}\boldsymbol{P}\boldsymbol{U}^{-1} & \boldsymbol{0}\\ \boldsymbol{0} & -\mu_c^2\boldsymbol{I}\end{bmatrix}\prec 0. \tag{56}$$

Pre- and post-multiplying it respectively by diag$(\boldsymbol{U}^T,\boldsymbol{I})$ and diag$(\boldsymbol{U},\boldsymbol{I})$ and then applying Lemma 1 gives

$$\begin{bmatrix}\boldsymbol{U}^T\boldsymbol{U}-\boldsymbol{P} & \boldsymbol{0} & \boldsymbol{U}^T\tilde{\boldsymbol{X}}_k^T\\ \boldsymbol{0} & -\mu_c^2\boldsymbol{I} & \tilde{\boldsymbol{Z}}^T\\ \tilde{\boldsymbol{X}}_k\boldsymbol{U} & \tilde{\boldsymbol{Z}} & \boldsymbol{P}-\boldsymbol{U}-\boldsymbol{U}^T\end{bmatrix}\prec 0. \tag{57}$$

Subsequently, applying the Schur complement gives

$$\begin{bmatrix}-\boldsymbol{P} & \boldsymbol{0} & \boldsymbol{U}^T\tilde{\boldsymbol{X}}_k^T & \boldsymbol{U}^T\\ \boldsymbol{0} & -\mu_c^2\boldsymbol{I} & \tilde{\boldsymbol{Z}}^T & \boldsymbol{0}\\ \tilde{\boldsymbol{X}}_k\boldsymbol{U} & \tilde{\boldsymbol{Z}} & \boldsymbol{P}-\boldsymbol{U}-\boldsymbol{U}^T & \boldsymbol{0}\\ \boldsymbol{U} & \boldsymbol{0} & \boldsymbol{0} & -\boldsymbol{I}\end{bmatrix}\prec 0. \tag{58}$$

Substituting

$$\tilde{\boldsymbol{X}}_k\boldsymbol{U}=\tilde{\boldsymbol{A}}_k\boldsymbol{U}-\boldsymbol{B}\boldsymbol{K}_c\boldsymbol{U}=\tilde{\boldsymbol{A}}_k\boldsymbol{U}-\boldsymbol{B}\boldsymbol{N}, \tag{59}$$

completes the proof. ∎

In much the same way as for the estimator design, solving (48) is equivalent to (for $i=1,\ldots,N$)

$$\begin{bmatrix}-\boldsymbol{P} & \boldsymbol{0} & \boldsymbol{U}^T\tilde{\boldsymbol{A}}_i^T-\boldsymbol{N}^T\boldsymbol{B}^T & \boldsymbol{U}^T\\ \boldsymbol{0} & -\mu_c^2\boldsymbol{I} & \tilde{\boldsymbol{Z}}^T & \boldsymbol{0}\\ \tilde{\boldsymbol{A}}_i\boldsymbol{U}-\boldsymbol{B}\boldsymbol{N} & \tilde{\boldsymbol{Z}} & \boldsymbol{P}-\boldsymbol{U}-\boldsymbol{U}^T & \boldsymbol{0}\\ \boldsymbol{U} & \boldsymbol{0} & \boldsymbol{0} & -\boldsymbol{I}\end{bmatrix}\prec 0. \tag{60}$$

Finally, the controller gain matrix is obtained as follows:

$$\boldsymbol{K}_c=\boldsymbol{N}\boldsymbol{U}^{-1}. \tag{61}$$

To recapitulate briefly, the FTC, which is able to compensate all sensor faults can be illustrated as in Fig. 1.

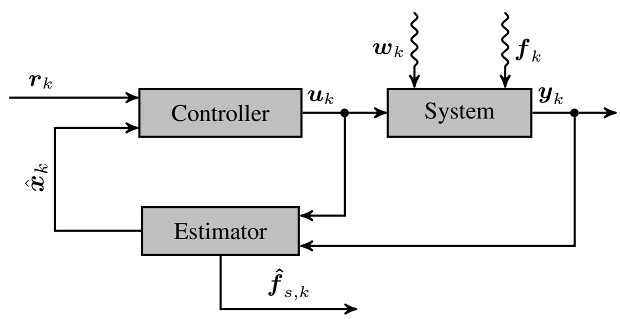

Fig. 1. Sensor fault-tolerant control scheme.

4. Illustrative example

To verify the proposed approach, a twin-rotor aero-dynamical system (Fig. 2) is employed. Such a system is designed to simulate the flight object in laboratory conditions. The system can be described by a highly non-linear model with cross coupled axes by using the following equations:

$$\frac{\mathrm{d}\omega_v}{\mathrm{d}t} = \frac{k_b k_2}{J_{mr} R_b} u_v - \left(\frac{B_{mr}}{J_{mr}} + \frac{k_b^2}{J_{mr} R_b} \right) \omega_v - \frac{f_4(\omega_v)}{J_{mr}}, \tag{62}$$

$$\begin{aligned}\frac{\mathrm{d}\Omega_v}{\mathrm{d}t} &= \frac{l_m f_5(\omega_v) + kg\Omega_h f_5(\omega_v)\cos(\theta_v) - k_{ov}\Omega_v}{J_v} \\ &+ \frac{g\left((K_A - K_B)\cos(\theta_v) - K_C \sin(\theta_v)\right)}{J_v} \\ &- \frac{\Omega_h^2 K_H \sin(\theta_v)\cos(\theta_v)}{J_v} \\ &+ \frac{k_t\left(\frac{k_a k_1}{R_a} u_h - \left(B_{tr} + \frac{k_a^2}{R_a}\right)\omega_h - f_1(\omega_h)\right)}{J_v J_{tr}},\end{aligned} \tag{63}$$

$$\frac{\mathrm{d}\theta_v}{\mathrm{d}t} = \Omega_v, \tag{64}$$

$$\frac{\mathrm{d}\omega_h}{\mathrm{d}t} = \frac{k_a k_1}{J_{tr} R_a} u_h - \left(\frac{B_{tr}}{J_{tr}} + \frac{k_a^2}{J_{tr} R_a} \right) \omega_h - \frac{f_1(\omega_h)}{J_{tr}}, \tag{65}$$

$$\begin{aligned}\frac{\mathrm{d}\Omega_h}{\mathrm{d}t} &= \frac{k_{oh} f_2(\omega_h)\cos(\theta_v) - k_{oh}\Omega_h - f_3(\theta_h) + f_6(\theta_v)}{\Phi} \\ &+ \frac{k_m \omega_v \sin(\theta_v)\Omega_v\left(-\Phi - 2K_E\cos^2(\theta_v)\right)}{(\Phi)^2} \\ &+ \frac{k_m \sin(\theta_v)\left(\frac{k_b k_2}{R_b} u_v - \left(B_{mr} + \frac{k_b^2}{R_b}\right)\omega_v - f_4(\omega_v)\right)}{J_{mr}\Phi},\end{aligned} \tag{66}$$

$$\frac{\mathrm{d}\theta_h}{\mathrm{d}t} = \Omega_h, \tag{67}$$

where $\Phi = K_D \cos^2(\theta_v) + K_E \sin^2(\theta_v) + K_F$, ω_v, Ω_v, θ_v, ω_h, Ω_h and θ_h are the rotational velocity of the main rotor, the angular velocity around horizontal axes, the pitch angle of the beam, the rotational velocity of the tail rotor, angular velocity around vertical axes and the yaw angle of the beam, respectively. The system state vector is

$$\boldsymbol{x} = \left[\omega_v^T, \Omega_v^T, \theta_v^T, \omega_h^T, \Omega_h^T, \theta_h^T\right]^T,$$

and the system input vector is

$$\boldsymbol{u} = \left[u_v^T, u_h^T\right]^T,$$

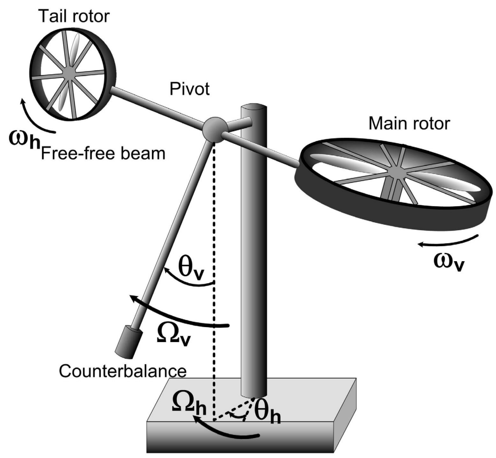

Fig. 2. Twin-rotor aero-dynamical system.

where u_v and u_h are the voltages of the main and tail rotors. The rest of the parameters are inherited from (Rotondo *et al.*, 2013).

The non-linear model, which describes the behaviour of the system, has been discretized with a sampling time $T_s = 0.01$ [s] which leads to the state-space representation (1)–(2). It is worth to emphasize that the angular velocity around both, vertical and horizontal axes were not measured directly during the experiment, which implies the output equation

$$\boldsymbol{C} = \begin{bmatrix} 1 & 0 & 0 & 0 & 0 & 0 \\ 0 & 0 & 1 & 0 & 0 & 0 \\ 0 & 0 & 0 & 1 & 0 & 0 \\ 0 & 0 & 0 & 0 & 0 & 1 \end{bmatrix}. \tag{68}$$

Moreover, consider a fault scenario

$$\boldsymbol{f}_{s,k} = \left[\boldsymbol{f}_{s,1,k}^T, \boldsymbol{f}_{s,3,k}^T, \boldsymbol{f}_{s,4,k}^T, \boldsymbol{f}_{s,6,k}^T\right]^T,$$

with

$$\begin{aligned}\boldsymbol{f}_{s,1,k} &= \begin{cases} \boldsymbol{y}_{1,k} - 192, & 3000 \le k \le 12000, \\ 0, & \text{otherwise}, \end{cases} \\ \boldsymbol{f}_{s,3,k} &= \begin{cases} \boldsymbol{y}_{2,k} - 0.2, & 5000 \le k \le 10000, \\ 0, & \text{otherwise}, \end{cases} \\ \boldsymbol{f}_{s,4,k} &= \begin{cases} \boldsymbol{y}_{4,k} - 384, & 6000 \le k \le 9000, \\ 0, & \text{otherwise}, \end{cases} \\ \boldsymbol{f}_{s,6,k} &= \begin{cases} \boldsymbol{y}_{6,k} + 0.1, & 8000 \le k \le 11000, \\ 0, & \text{otherwise}, \end{cases}\end{aligned} \tag{69}$$

which means that intermittent faults occurred in all of four sensors. In the above scenario, the faults overlap each other, and at some time instances all sensors are faulty. This means that all sensors give wrong measurements, simultaneously.

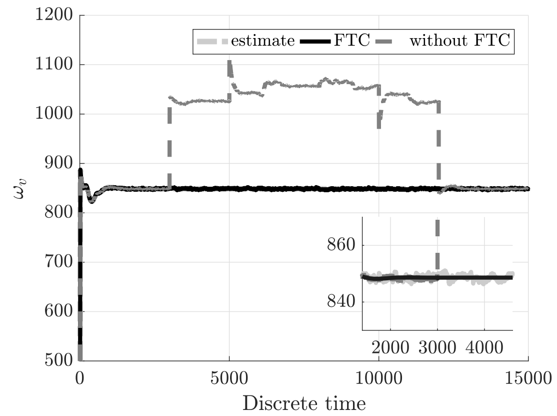

Fig. 3. State variable $\boldsymbol{x}_1$ and its estimate $\hat{\boldsymbol{x}}_1$.

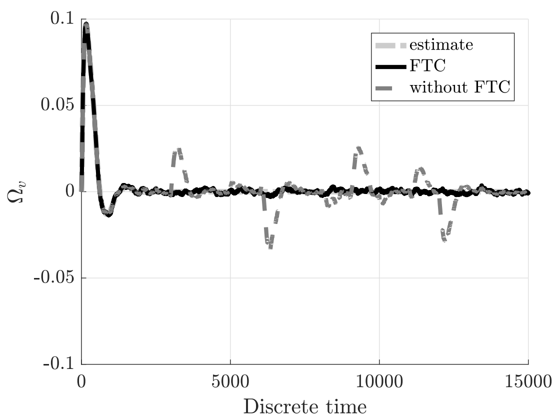

Fig. 4. State variable $\boldsymbol{x}_2$ and its estimate $\hat{\boldsymbol{x}}_2$.

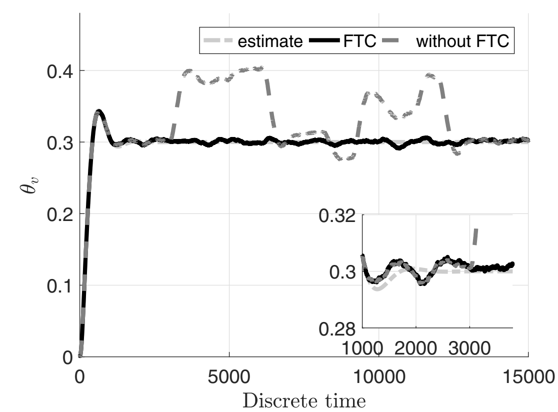

Fig. 5. State variable $\boldsymbol{x}_3$ and its estimate $\hat{\boldsymbol{x}}_3$.

It should be noted that the results presented in this section are based on the simulations with the mathematical model (62)–(67). The main reason behind it is that it is hard to introduce sensor and actuator faults within the laboratory counterpart of (62)–(67). Assume that the initial state for the system as well as for the observer are $\boldsymbol{x}_0 = [0, 0, 0.001, 0, 0, 0.001]$ and $\hat{\boldsymbol{x}}_0 = [0, 0, 0.01, 0, 0, 0.01]$, respectively, while the fault estimate is initialized by $\hat{\boldsymbol{f}}_{s,0} = [0, 0, 0, 0]$.

By solving a set of LMIs (32) described in Section 3.1, the following observer gain matrices have been obtained:

$$\boldsymbol{K}_x = 10^{-4}\begin{bmatrix} -0.0360 & 0.0014 & 0.0004 & 0.0000 \\ 0.0053 & -0.0080 & 0.0014 & 0.0272 \\ -0.0020 & 0.1961 & -0.0003 & 0.0048 \\ 0.0016 & -0.0023 & 0.0802 & 0.0081 \\ -0.0031 & 0.0237 & -0.0525 & 0.5181 \\ 0.0026 & 0.0072 & 0.0186 & 0.3602 \end{bmatrix}, \tag{70}$$

$$\boldsymbol{K}_s = \begin{bmatrix} 0.9987 & 0.0000 & -0.0000 & -0.0000 \\ 0.0000 & 0.9995 & -0.0000 & 0.0000 \\ -0.0000 & 0.0000 & 0.9991 & -0.0000 \\ 0.0000 & 0.0000 & -0.0001 & 0.9996 \end{bmatrix}. \tag{71}$$

Solving a set of LMIs (60) described in Section 3.2, the following controller gain matrix has been obtained:

$$\boldsymbol{K}_c = \left[\begin{matrix} -35.6089 & -8.7674 & -4.4345 \\ -0.2607 & -21.6470 & -1.8907 \end{matrix}\right. \quad \left.\begin{matrix} 0.2404 & -0.6062 & 1.8596 \\ -118.5292 & -53.2380 & 26.7607 \end{matrix}\right], \tag{72}$$

The control goal was to achieve appropriate pitch and yaw angles. Thus, the reference signal during the experiment was

$$\boldsymbol{r}_k = \begin{bmatrix} 0.3 \\ 0.2 \end{bmatrix}. \tag{73}$$

Figures 3–8 present the response of the system in the faulty case. The black solid line in these graphs represents the system state with FTC and the dashed line represents the system state controlled by a classical robust controller without fault tolerance. Moreover, the dash-dot line represent the state estimate. The controlled state variables θ_v and θ_h are presented in Figs. 5 and 8, respectively. It is easy to see that the system with FTC is following the reference signal (grey line) in contrast to the response without FTC. It should be also mentioned that it was needed about 20 [s] for the pitch angle and about 15 [s] for the yaw angle to reach the reference signal. The system is controlled properly even in case of faults thanks to the knowledge about the fault estimate $\hat{\boldsymbol{f}}_{s,k}$ and, as a consequence the fault-free state estimate $\hat{\boldsymbol{x}}_k$. In the regular control without FTC, the values measured by the faulty sensors are assumed as correct ones and the system is guided according to the measurements. This may lead to the total failure of the system. Figures 9–12 show comparisons between real and estimated faults. It is easy to see that the estimated faults are pursuing the real ones highly satisfactory. This implies the accuracy of the state estimate. Finally, Figs. 13 and 14 present the control signal for the main and tail rotor, respectively, in the range from -1 to 1. It can be seen that the control signal changes

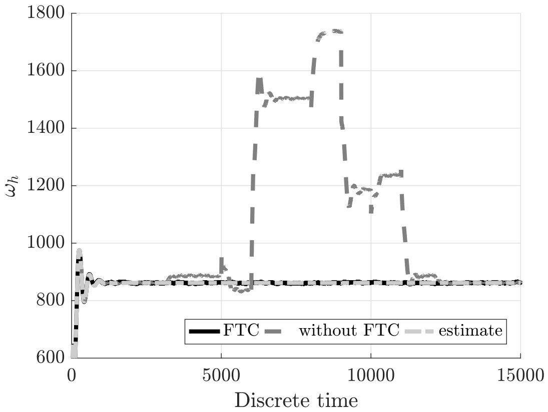

Fig. 6. State variable $\boldsymbol{x}_4$ and its estimate $\hat{\boldsymbol{x}}_4$.

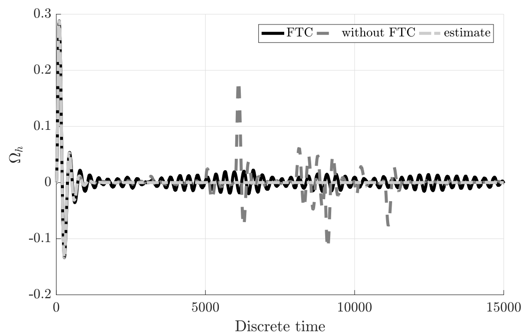

Fig. 7. State variable $\boldsymbol{x}_5$ and its estimate $\hat{\boldsymbol{x}}_5$.

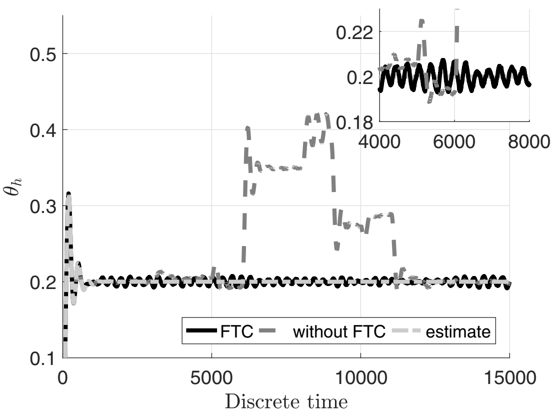

Fig. 8. State variable $\boldsymbol{x}_6$ and its estimate $\hat{\boldsymbol{x}}_6$.

adequately to what has been measured in the case without fault tolerance while it is maintained at a constant level in the case of FTC. This remains in contrast to the results obtained without fault tolerance. The obtained results confirm that FTC allows controlling the system correctly even in the case of sensor faults.

5. Conclusions

The main aim of the paper was to handle the system control problem while the sensor faults occur once. The strategy for simultaneous estimation of the state and the fault was proposed. The presented observer was able to estimate the fault for all of the sensors in the system simultaneously and thanks to that it is easy to compensate the fault influence. The design strategy for the observer as well as for the controller was based on the $\mathcal{H}_\infty$ approach which boils down to solving a set of LMIs. It can be easily used in fault diagnosis for linear as well as non-linear LPV-like systems. The final part of the paper shows an illustrative example with an application to the twin-rotor aero-dynamical system. The achieved results confirm the correctness and effectiveness of the proposed approach.

References

Aouaouda, S. Chadli, M., Shi, P. and Karimi, H. (2015). Discrete-time H_/H-inf sensor fault detection observer design for nonlinear systems with parameter uncertainty, *International Journal of Robust and Nonlinear Control* **25**(3): 339–361.

Byrski, J. and Byrski, W. (2016). A double window state observer for detection and isolation of abrupt changes in parameters, *International Journal of Applied Mathematics and Computer Science* **26**(3): 585–602, DOI: 10.1515/amcs-2016-0041.

Cai, J., Ferdowsi, H. and Sarangapani, J. (2016). Model-based fault detection, estimation, and prediction for a class of linear distributed parameter systems, *Automatica* **66**: 122–131.

de Oliveira, M.C., Bernussou, J. and Geromel, J.C. (1999). A new discrete-time robust stability condition, *Systems & Control Letters* **37**(4): 261–265.

Defoort, M., Veluvolu, K. and Rath, J.and Djemai, M. (2016). Adaptive sensor and actuator fault estimation for a class of uncertain Lipschitz nonlinear systems, *International Journal of Adaptive Control and Signal Processing* **30**(2): 271–283.

Foo, G., Zhang, X. and Vilathgamuwa, M. (2013). A sensor fault detection and isolation method in interior permanent-magnet synchronous motor drives based on an extended Kalman filter, *IEEE Transactions on Industrial Electronics* **60**(8): 3485–3495.

Ha, Q.P. and Trinh, H. (2004). State and input simultaneous estimation for a class of nonlinear systems, *Automatica* **40**(10): 1779–1785.

He, Q. and Liu, J. (2014). Sliding mode observer for a class of globally Lipschitz non-linear systems with time-varying delay and noise in its output, *IET Control Theory & Applications* **8**(14): 1328–1336.

Isermann, R. (2011). *Fault-Diagnosis Applications. Model-Based Condition Monitoring: Actuators, Drives, Machinery, Plants, Sensors, and Fault-Tolerant Systems*, Springer, Berlin/Heidelberg.

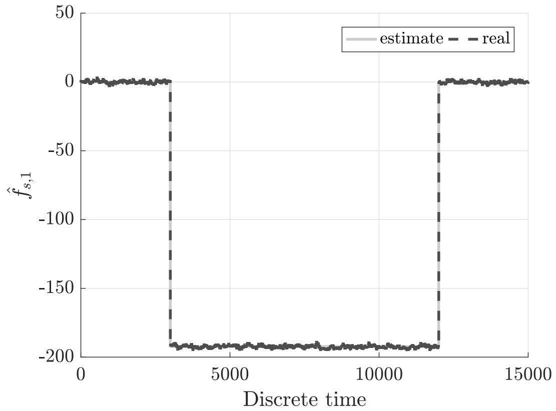

Fig. 9. Fault $\boldsymbol{f}_{s,1}$ and its estimate $\hat{\boldsymbol{f}}_{s,1}$.

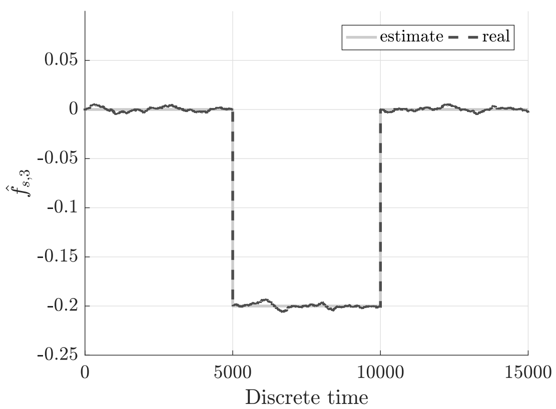

Fig. 10. Fault $\boldsymbol{f}_{s,3}$ and its estimate $\hat{\boldsymbol{f}}_{s,3}$.

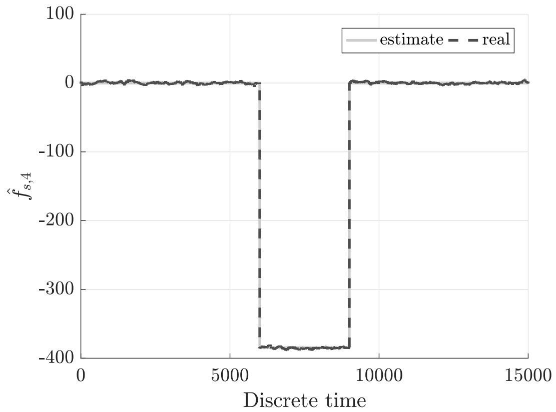

Fig. 11. Fault $\boldsymbol{f}_{s,4}$ and its estimate $\hat{\boldsymbol{f}}_{s,4}$.

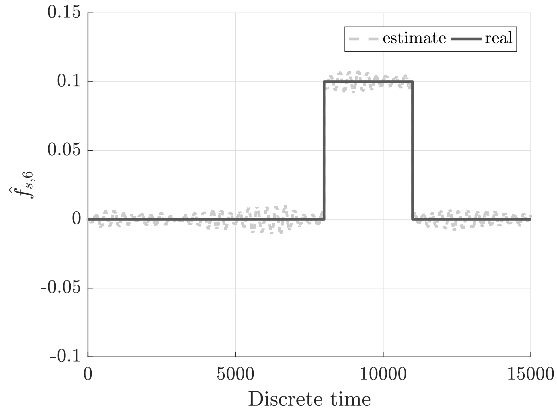

Fig. 12. Fault $\boldsymbol{f}_{s,6}$ and its estimate $\hat{\boldsymbol{f}}_{s,6}$.

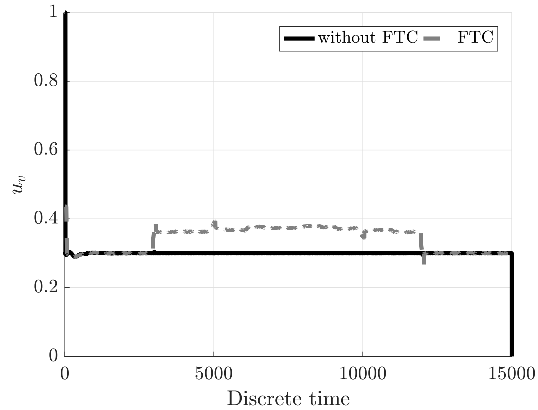

Fig. 13. Control signal for the main rotor.

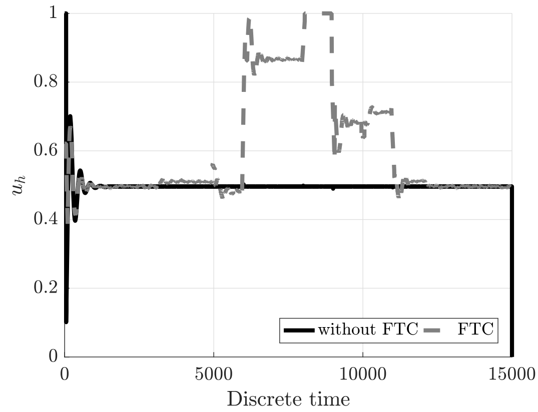

Fig. 14. Control signal for the tail rotor.

Khalil, H. and Praly, L. (2014). High-gain observers in nonlinear feedback control, *International Journal of Robust and Nonlinear Control* **24**(6): 993–1015.

Li, H. and Fu, M. (1997). A linear matrix inequality approach to robust H_∞ filtering, *IEEE Transactions on Signal Processing* **45**(9): 2338–2350.

Li, L., Yang, Y., Zhang, Y. and Ding, S. (2014). Fault estimation of one-sided Lipschitz and quasi-one-sided Lipschitz systems, *33rd Chinese Control Conference (CCC), Nanjing, China*, pp. 2574–2579.

Löfberg, J. (2004). YALMIP: A toolbox for modeling and optimization in Matlab, *Proceedings of the CACSD Conference, New Orleans, LA, USA*, pp. 284–289.

López-Estrada, F.-R., Ponsart, J.-C., Theilliol, D., Astorga-Zaragoza, C.-M., and Camas-Anzueto, J.-L. (2015). Robust sensor fault estimation for descriptor-LPV systems with unmeasurable gain scheduling functions: Application to an anaerobic bioreactor, *International Journal of Applied Mathematics and Computer Science* **25**(2): 233–244, DOI: 10.1515/amcs-2015-0018.

Mahmoud, M., Jiang, J. and Zhang, Y. (2003). *Active Fault Tolerant Control Systems: Stochastic Analysis and Synthesis*, Springer, Berlin/Heidelberg.

Majdzik, P., Akielaszek-Witczak, A., Seybold, L., Stetter, R. and Mrugalska, B. (2016). A fault-tolerant approach to the control of a battery assembly system, *Control Engineering Practice* **55**: 139–148.

Mrugalski, M. (2014). *Advanced Neural Network-based Computational Schemes for Robust Fault Diagnosis*, Springer, Berlin/Heidelberg.

Nguyen, M.C. and Trinh, H. (2016a). Reduced-order observer design for one-sided Lipschitz time-delay systems subject to unknown inputs, *IET Control Theory & Applications* **10**(10): 1097–1105.

Nguyen, M.C. and Trinh, H. (2016b). Unknown input observer design for one-sided Lipschitz discrete-time systems subject to time-delay, *Applied Mathematics and Computation* **286**: 57–71.

Pourbabaee, B., Meskin, N. and Khorasani, K. (2016). Sensor fault detection, isolation, and identification using multiple-model-based hybrid Kalman filter for gas turbine engines, *IEEE Transactions on Control Systems Technology* **24**(4): 1184–1200.

Rotondo, D., Nejjari, F. and Puig, V. (2013). Quasi-LPV modeling, identification and control of a twin rotor MIMO system, *Control Engineering Practice* **21**(6): 829–846.

Seron, M.M. and De Doná, J.A. (2015). Robust fault estimation and compensation for LPV systems under actuator and sensor faults, *Automatica* **52**: 294 – 301.

Seybold, L., Witczak, M., Majdzik, P. and Stetter, R. (2015). Towards robust predictive fault-tolerant control for a battery assembly system, *International Journal of Applied Mathematics and Computer Science* **25**(4): 849–862, DOI: 10.1515/amcs-2015-0061.

Song, J.and He, S. (2015). Robust finite-time H-inf control for one-sided Lipschitz nonlinear systems via state feedback and output feedback, *Journal of the Franklin Institute* **352**(8): 3250–3266.

Tabatabaeipour, S.M. and Bak, T. (2014). Robust observer-based fault estimation and accommodation of discrete-time piecewise linear systems, *Journal of the Franklin Institute* **351**(1): 277–295.

Witczak, M. (2014). *Fault Diagnosis and Fault-Tolerant Control Strategies for Non-Linear Systems: Analytical and Soft Computing Approaches*, Springer, Heidelberg.

Witczak, M., Buciakowski, M., Puig, V., Rotondo, D. and Nejjari, F. (2015). An LMI approach to robust fault estimation for a class of nonlinear systems, *International Journal of Robust and Nonlinear Control* **26**(7): 1530–1548.

Zemouche, A. and Boutayeb, M. (2006). Observer design for Lipschitz non-linear systems: The discrete time case, *IEEE Transactions on Circuits and Systems* **53**(8): 777–781.

Zemouche, A., Boutayeb, M. and Bara, G.I. (2008). Observers for a class of Lipschitz systems with extension to H_∞ performance analysis, *Systems & Control Letters* **57**(1): 18–27.

Zhang, J., Swain, A. and Nguang, S. (2014a). Robust H-inf adaptive descriptor observer design for fault estimation of uncertain nonlinear systems, *Journal of the Franklin Institute* **351**(11): 5162–5181.

Zhang, W., Su, H., Su, S. and Wang, D. (2014b). Nonlinear H-inf observer design for one-sided Lipschitz systems, *Neurocomputing* **145**: 505–511.

Zhang, W., Su, H., Zhu, F. and Azar, G. (2015). Unknown input observer design for one-sided Lipschitz nonlinear systems, *Nonlinear Dynamics* **79**(2): 1469–1479.

Marcin Pazera was born in Poland in 1990. He received the MSc degree in automatic control and robotics from the University of Zielona Góra (Poland) in 2015. He is currently a PhD student at the Institute of Control and Computation Engineering, University of Zielona Góra. His present research interests include fault detection and isolation (FDI), fault-tolerant control (FTC), as well as experimental design and control theory.

Mariusz Buciakowski received his MSc degree in automatic control and robotics in 2013 from the Faculty of Electrical Engineering, Computer Science and Telecommunications of the University of Zielona Góra. Currently he is a PhD student at this faculty. His present research interests include robust control, fault tolerant control, model predictive control, and practical verification of developed algorithms based on embedded systems and PLC controllers.

Marcin Witczak was born in Poland in 1973, received the MSc degree in electrical engineering from the University of Zielona Góra (Poland), the PhD degree in automatic control and robotics from the Wrocław University of Technology (Poland), and the DSc degree in electrical engineering from the University of Zielona Góra, in 1998, 2002 and 2007, respectively. In 2015 he received a full professorial title. He is a professor of automatic control and robotics at the Institute of Control and Computation Engineering, University of Zielona Góra. His current research interests include computational intelligence, fault detection and isolation (FDI), fault-tolerant control (FTC), as well as experimental design and control theory. Marcin Witczak has published more than 160 papers in international journals and conference proceedings. He is an author of 4 monographs and 30 book chapters. Since 2015, he has been a member of the Committee on Automatic Control and Robotics of the Polish Academy of Sciences. As of 2018, he is also an associate editor of *ISA Transactions*.

Received: 17 March 2017
Revised: 5 October 2017
Re-revised: 11 January 2018
Accepted: 13 January 2018